Am J Transl Res 2015;7(7):1214-1226
www.ajtr.org /ISSN:1943-8141/AJTR0010345

Original Article

Transplantation of bradykinin-preconditioned human endothelial progenitor cells improves cardiac function via enhanced Akt/eNOS phosphorylation and angiogenesis

Zu-Long Sheng*, Yu-Yu Yao*, Ye-Fei Li, Cong Fu, Gen-Shan Ma

*Department of Cardiology, Zhongda Hospital, Medical School of Southeast University, 87 Dingjiaqiao, Nanjing, Jiangsu, 210009, China. *Equal contributors.*

Received March 21, 2015; Accepted July 14, 2015; Epub July 15, 2015; Published July 30, 2015

Abstract: This study determines whether preconditioning (PC) of human endothelial progenitor cells (hEPCs) with bradykinin promotes infarcted myocardium repair via enhanced activation of B2 receptor (B2R)-dependent Akt/eNOS and increased angiogenesis. hEPCs with or without bradykinin preconditioning (BK-PC) were transplanted into a nude mouse model of acute myocardial infarction. Survival of transplanted cells was assessed using DiD-labeled hEPCs. Infarct size, cardiac function, and angiogenesis were measured 10 d after transplantation. Akt, eNOS, and vascular endothelial growth factor (VEGF) expressions in cardiac tissues were detected by western blotting, and NO production was determined using an NO assay kit. The cell migration and tube formation in cultured hEPCs were determined using transwell chamber and matrigel tube formation assays, respectively. The VEGF levels in the cell supernatant were measured using an enzyme-linked immunosorbent assay kit. BK-PC-hEPCs improved cardiac function, decreased infarct size, and promoted neovascularization 10 d following transplantation. PC increased Akt and eNOS phosphorylation, VEGF expression, and NO production in the ischemic myocardium. The effects of BK-PC were abrogated by HOE140 (B2R antagonist) and LY294002 (Akt antagonist). PC increased hEPC migration, tube formation, and VEGF levels *in vitro.* Activation of B2R-dependent Akt/eNOS phosphorylation by BK-PC promotes hEPC neovascularization and improves cardiac function following transplantation.

Keywords: Bradykinin, endothelial progenitor cells, myocardial infarction, preconditioning, neovascularization

Introduction

Myocardial infarction (MI) remains a major cause of morbidity and mortality worldwide. Therapeutic angiogenesis is a promising concept with significant potential clinical applications for the treatment of patients with ischemia [1, 2]. An increasing body of evidence from a wide range of experimental animal studies and clinical trials suggests that endothelial progenitor cells (EPCs) participate in the process of neovascularization and tissue repair, which leads to the enhanced recovery of ischemic myocardium [3, 4]. Several studies have demonstrated that the therapeutic effects of EPCs may result from the growth factors secreted by EPCs, the differentiation into endothelial cells (ECs), and the incorporation into sites of active neovascularization [5-7]. However, transplantation of autologous EPCs has numerous limitations, including the limited supply of expanded progenitors, the pathological microenvironment, and the low proportion of intravenously injected cells that successfully accumulate at sites of tissue damage [8]. Therefore, developing novel proangiogenic strategies that improve revascularization of ischemic tissues is clinically significant.

Preconditioning (PC) of stem cells is an attractive strategy for improving revascularization of ischemic tissues. Hypoxically preconditioned human peripheral blood mononuclear cells improve blood flow in hindlimb ischemia xenograft model [9], and preconditioning of bone marrow mesenchymal stem cells by prolyl

hydroxylase inhibition enhances cell survival and angiogenesis in vitro and after transplantation into the ischemic heart of rats [10]. Moreover, the PC of EPCs with stromal-derived factor-1 (SDF-1) has been reported to enhance angiogenesis, thus augmenting the efficiency of cell therapy for ischemic vascular diseases [11].

Bradykinin (BK), one of the major metabolites in the tissue kallikrein-kinin system, plays a vital role in regulating the tolerance of an ischemic heart [12]. BK has been widely known as an endogenous protective factor that reduces infarct size and improves post-ischemic contractile function [13]. BK is one of the triggers of ischemic preconditioning (IPC) [14] and limits the infarct size in the ischemic heart during the late phase of IPC by activating B2R [15]. Bradykinin preconditioning (BK-PC) improves the recovery of ventricular and coronary vascular function via nitric oxide-dependent mechanisms [16].

However, the BK-PC of stem cells prior to transplantation has not been previously investigated. In this study, we postulated that PC-hEPCs with BK transplantation will significantly enhance neovascularization and promote infarcted myocardium repair.

Materials and methods

Isolation, culture, and characterization of hEPCs

Human umbilical cord blood was obtained from Zhongda Hospital in accordance with an institutional review board-approved protocol. All selected pregnant women were healthy and signed an informed consent. The obtained human umbilical cord blood was diluted to a 1:1 ratio in phosphate-buffered saline (PBS) in a similar manner as used in previous studies [17]. The mononuclear cell fraction was obtained from a Lymphoprep density gradient (Sigma, St. Louis, MO, USA) after centrifugation, washed twice in PBS, and centrifuged. The cell pellet was suspended in endothelial basal growth medium (EBM-2) supplemented with EGM-2 MV SingleQuots and 5% heat inactivated fetal bovine serum (FBS) (EGM-2, Lonza, Walkersville, MD, USA). The solution was then plated in a T-25 culture flask coated with 10 μg/mL human plasma fibronectin (FN, Millipore, Bedford, MA, USA). After removing unbound cells at 96 h, the bound cell fraction was maintained in culture by using EGM-2. Spindle-shaped cells were observed after 7 d. Colonies of endothelial-like cells were grown to confluence and subsequently trypsinized and paved uniformly in a new T-25 culture flask as the first passage. The medium was changed every 3 d. At 80% confluence, cells were harvested with 0.25% trypsin and passaged at a ratio of 1:2. Subsequent passages were performed similarly. Passages 3 hEPCs to 6 hEPCs were used in this study.

Cells were primarily characterized by phase contrast microscopy to evaluate the cobblestone morphology. Cells were incubated with 1, 1'-dioctadecyl 3,3,3',3'-tetra-methylindo-carbocyanine-labeled acetylated low-density lipoprotein (DiI -acLDL, Invitrogen, Carlsbad, California, USA) for 4 h at 37°C. Lectin binding was analyzed by using fluorescein isothiocyanate (FITC)-conjugated UEA-1-lectin (Sigma), and the cells were examined under a fluorescence microscope (Nikon Corporation). Immunofluorescence staining was also utilized to determine the expression of the progenitor lineage marker CD34 (BD Biosciences, Bedford, Massachusetts, USA), the endothelial lineage markers VEGFR2 (KDR, BD Biosciences) and CD105 (Santa Cruz), the myeloid marker CD68 (BD Biosciences), the leukocyte marker CD45 (BD Biosciences), and the B2R expression (BD Biosciences). Flow cytometry was used to analyze B1R and B2R expressions.

Nude mouse model of acute MI and transplantation of labeled hEPCs

All animal studies were approved by the Institutional Animal Care and Use Committee of Southeast University. The recipient male nude mice (20 g to 22 g, weight) were intraperitoneally anesthetized with 45 mg/kg of pentobarbital, intubated, and then ventilated at 110 breaths per min. The left anterior descending coronary artery was proximally ligated with 8-0 silk suture via left thoracotomy incision. After 10 min, the animals were grouped and intramyocardially injected with 30 μl of one of the following: basal medium without hEPCs (Con group), basal medium containing 1×10^6 non-PC hEPCs (EPCs group), bradykinin-preconditioned hEPCs (BK-PC-hEPCs; BK PC group), BK-PC-hEPCs pretreated with HOE140 (BK PC/

HOE group), and LY294002 (BK PC/LY group). The injections were performed at multiple sites (average of 3 to 4 sites/animal) in the free wall of the LV under direct vision. After the chests of the animals were sutured, the animals were allowed to recover.

Prior to heart transplantation, a cell suspension containing 1×10^6 hEPCs was labeled with carbocyanine near-infrared dye 1, 1'-dioctadecyl-3,3,3',3'-tetramethylindodicarbocyanine,4-chlorobenzenesulfonate salt (DiD; Invitrogen, Carlsbad, CA, USA) according to the manufacturer's instructions.

Echocardiographic analysis and heart/body weight measurement

The day 10 group was evaluated for cardiac function by using transthoracic echocardiography prior to sacrifice (Vevo 770TM; Visual Sonic, Toronto, Canada). Left parasternal short-axis two-dimensional M-mode images at the level of papillary muscles were recorded by using a 30 MHz linear transducer. Left ventricular end-diastolic volume (LVEDV), left ventricular end-systolic volume (LVESV), left ventricular internal diameter at end-diastole (LVIDd), and left ventricular internal diameter at end-systole (LVIDs) were measured at the anterior wall from the short-axis view just below the level of the papillary muscle. The left ventricular ejection fraction (LVEF) and left ventricular fractional shortening (LVFS) were calculated by using standard M-mode echocardiographic equations (EF = (LVEDV - LVESV) × 100%/LVEDV; FS = (LVIDd - LVIDs) × 100%/LVIDd). All measurements were averaged for five consecutive cardiac cycles and performed by an experienced examiner in a blinded fashion.

After determining the cardiac function via echocardiography, the heart was perfused with PBS and rapidly excised. After drying by using filter paper, the heart was weighed with an electronic balance. The heart weight/body weight index was calculated as heart weight/body weight × 100.

Histological analysis

For morphological analysis, 4 μm sections were obtained and subjected to Masson's trichrome staining by using a staining kit (Sigma) according to the manufacturer's instruction. The LV images of each slide were taken by using a Nikon E200 (Nikon Corporation) camera. The fibrosis and total LV area of each image were measured by using Image-Pro Plus. The percentage of the fibrotic area was calculated as fibrosis area/total LV area × 100.

Immunohistochemical analyses were performed to visualize the capillaries and small arteries in the border zone by using a kit according to the manufacturer's instructions (UniversalElite ABC, Vector). Primary antibodies against CD 31 (endothelial cell antigen, Santa Cruz Biotechnology, Santa Cruz, CA, USA 1:50 dilution) and α-smooth muscle actin (Santa Cruz, 1:200 dilution) were used. Capillaries were identified as having a diameter of < 20 μm and a layer of ECs without smooth muscle cells, whereas arterioles were identified as having a diameter of > 20 μm and < 100 μm with a layer of smooth muscle cells. Positively stained cells in five fields per section of the peri-infarct zone were counted to determine capillary density and arteriole density. A total of five sections per heart were analyzed by an investigator blinded to the treatment (n = 5 for each group).

Immunofluorescence colocalization studies

The transplanted animals were sacrificed 10 d following transplantation, immediately after *ex vivo* imaging. Tissues were frozen in optimum cutting temperature compound (OCT compound, Miles Laboratories, Naperville, IL, USA) and sectioned into 5 μm samples by using a cryostat (LeiCa CM1950, Nussloch, Germany). The cryostat sections of the peri-infarct region of the hearts were fixed with acetone for 20 min, washed in PBS, and subsequently stained for antibodies against CD31 (Santa Cruz, 1:50 dilution) and α-smooth muscle actin (Santa Cruz, 1:50 dilution). The sections were visualized by using fluorescence-labeled secondary antibodies (Santa Cruz, 1:100 dilution). All sections were counterstained with 4',6-diamidino-2-phenylindole (DAPI) (Sigma). The multiple immunofluorescence-conjugated specimens were evaluated with a confocal microscope (FV-1000, Olympus, Tokyo, Japan).

Western blots analysis

Tissue samples (approximately 100 mg) taken from liquid nitrogen were homogenized in ice-cold RIPA lysis buffer with phenylmethanesulfonyl fluoride (10 mM, Shenergy Biocolor Bioscience and Technology Company, Shang-

hai, China). Extracts were cleared by centrifugation (16,000 × g at 4°C for 15 min), and the supernatants were collected. Protein concentration was determined by using a protein assay kit (Thermo scientific, Rockford, USA). Samples were mixed with sodium dodecyl sulfate (SDS)-denaturing sample buffer and separated through 10% SDS polyacrylamide gel electrophoresis gels. The proteins were transferred to a PVDF membrane by electrophoresis. The membrane was blocked and incubated overnight on a rocking platform at 4°C with antibodies against Akt, Phospho-Akt [Ser473], Phospho-eNOS [Ser1177] (1:1000, Cell Signaling, MA, USA), vascular endothelial growth factor (VEGF) (1:1000, Santa Cruz, CA, USA), as well as eNOS (1:1000, BD Biosciences) and glyceraldehyde 3-phosphate dehydrogenase (GAPDH) (1:1000 Kangchen Biology Inc., Shanghai, China). HRP-conjugated secondary antibodies were then incubated for 1 h and exposed with Molecular Imager ChemiDoc XRS System (Bio RAD CA, USA). Relative intensities of protein bands were analyzed by Image-Pro Plus 6.0 (Media Cybernetics, Silver Spring, MD, USA).

Measurement of NO release

The amount of NO in cardiac tissue was determined by using an NO assay kit (Beyotime, Shanghai, China) according to the manufacturer's protocol, as previously described [18]. Briefly, tissue samples from the risk area were rinsed, homogenized in deionized water (1:10, wt/vol), and centrifuged at 14,000 × g for 10 min. The absorbance at 550 nm was measured with a microplate reader (Bio RAD) after enzymatic conversion of the supernatant nitrate to nitrite by nitrate reductase. Supernatant NO levels were determined by colorimetric assay.

Transwell migration assay

The hEPCs were randomly assigned to the following six experimental groups: the Con group composed of non-PC hEPCs; the HOE140 and LY294002 groups (HOE group and LY group) composed of hEPCs incubated with either 150 nM of HOE140 (Sigma) or 10 μM of LY294002 (LY, Sigma) for 30 min independent of BK-PC; the BK-PC group composed of PC hEPCs incubated with 10 nM BK (Sigma) for 10 min; and the BK-PC/HOE and BK-PC/LY groups composed of PC hEPCs incubated with either 150 nM of HOE140 or 10 μM of LY294002 for 30 min prior to BK. At every step, three times of washes were applied with pre-warmed PBS to remove residual serum and drugs.

hEPC migration was evaluated by using a transwell migration assay. Briefly, 4×10^4 cells were suspended in 200 μL of RPMI-1640 medium supplemented with 1% FBS and placed in the upper chamber of an 8.0 μm pore size transwell (Millipore, Bedford, MA, USA). SDF-1 (100 ng/mL) was mixed with the medium (RPMI-1640 medium + 1% FBS) in the lower chamber. After incubation for 8 h at 37°C in 5% CO_2, the cells that failed to migrate were removed from the upper surface of the filters by using cotton swabs, and cells that migrated to the lower surface of the filters were stained with 0.1% crystal violet stain solution. Migration was determined by counting the cell number with a microscope (Nikon Corporation). The average number of migrating cells in five fields was taken as the cell migration number of the group.

Matrigel tube formation assay

hEPCs were randomly assigned to six experimental groups before the tube formation assay was performed. The growth factor-reduced matrigel (BD Biosciences) at 50 μl/well was laid into 96-well plates to solidify to analyze the capillary-like tube formation of EPCs. EPCs (passage 3) were seeded into six-well plates. EPCs 1×10^4) were resuspended in 200 μlL of EBM-2 without EGM-2 SingleQuots supplements and then plated on matrigel. After 18 h, tube images were obtained by using an inverted microscope. The degree of tube formation was quantified by measuring the length of tubes in three random fields from each well by using Image-Pro Plus (Media Cybernetics Inc., Carlsbad, CA, USA) and then calculated against control groups.

Measurement of vascular endothelial growth factor levels

The VEGF levels in the cell supernatant were measured by using an enzyme-linked immunosorbent assay kit (R&D Systems Inc., Minneapolis, MN, USA) according to the manufacturer's instructions.

Statistical analysis

Data were expressed as mean ± SEM. The data of the experimental groups were compared by

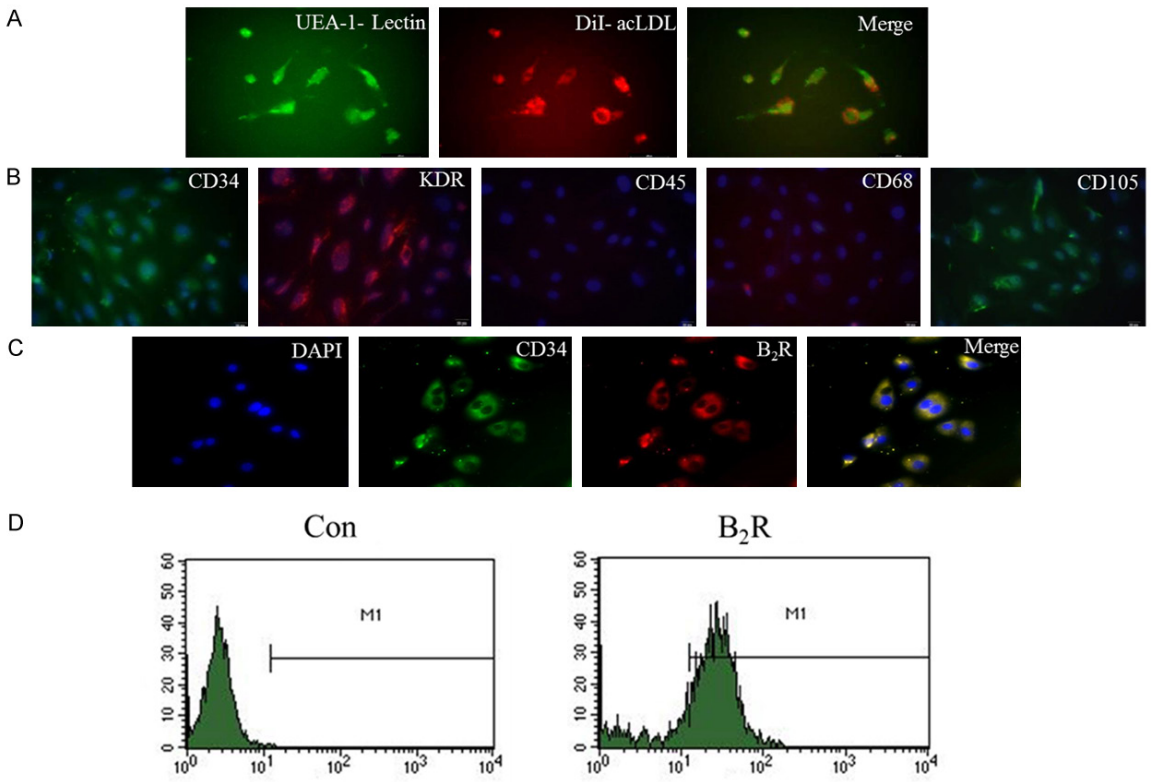

Figure 1. Characterization of cultured hEPCs and B2R expression in hEPCs. A. At 7 d following isolation, the adherent cells intensively took up acLDL and bound an endothelial-specific lectin, as assessed by using fluorescence microscopy (original magnification: 400 ×). B. The hEPCs of passage 3 were positive for CD34, KDR, and CD105, but negative for CD45 and CD68, as determined by immunofluorescence (original magnification: 400 ×). C. Co-localization of B2R with the progenitor lineage marker CD34 in the hEPCs of passage 3 (original magnification: 400 ×). D. B2R expression in hEPCs was detected via flow cytometry.

using one-way ANOVA and by Fisher's PLSD. Differences were considered statistically significant at $P < 0.05$.

Results

Characterization of hEPCs

The mononuclear cells derived from human umbilical cord blood were separated by using density gradient centrifugation and differentiated into "late-outgrowth EPCs" after a long culture period (three to six passages). The endothelial cell phenotype was characterized by assessing the acLDL-DiI uptake and FITC-conjugated UEA-1-lectin binding (**Figure 1A**). The hEPCs were positive for CD34, KDR, and CD105 but negative for CD45 and CD68 (**Figure 1B**). The cells were therefore confirmed as hEPCs. In addition, hEPCs expressed high levels of B2R and co-expressed B2R, as well as the EPC marker CD34 (**Figure 1C** and **1D**). The B1R expression in hEPCs was rarely detectable (data not shown).

Effects of BK-preconditioned hEPCs transplantation on cardiac function and infarct size after MI

Transthoracic echocardiographic examination was performed 10 d following cell delivery to evaluate cardiac function. The LVEF and LVFS were significantly reduced after MI, but were partially restored by transplantation of hEPCs and BK-PC-hEPCs (**Figure 2A** and **Table 1**). Moreover, a significant increase in both LVEF and LVFS in the BK-PC group was observed. However, no significant differences in LVEF and LVFS were observed among the EPCs, BK PC/HOE, and BK PC/LY groups. Impairments in contractility (left ventricular inner systolic diameter) and diastolic function (left ventricular inner diastolic diameter) after MI were significantly improved after BK-PC-hEPC transplanta-

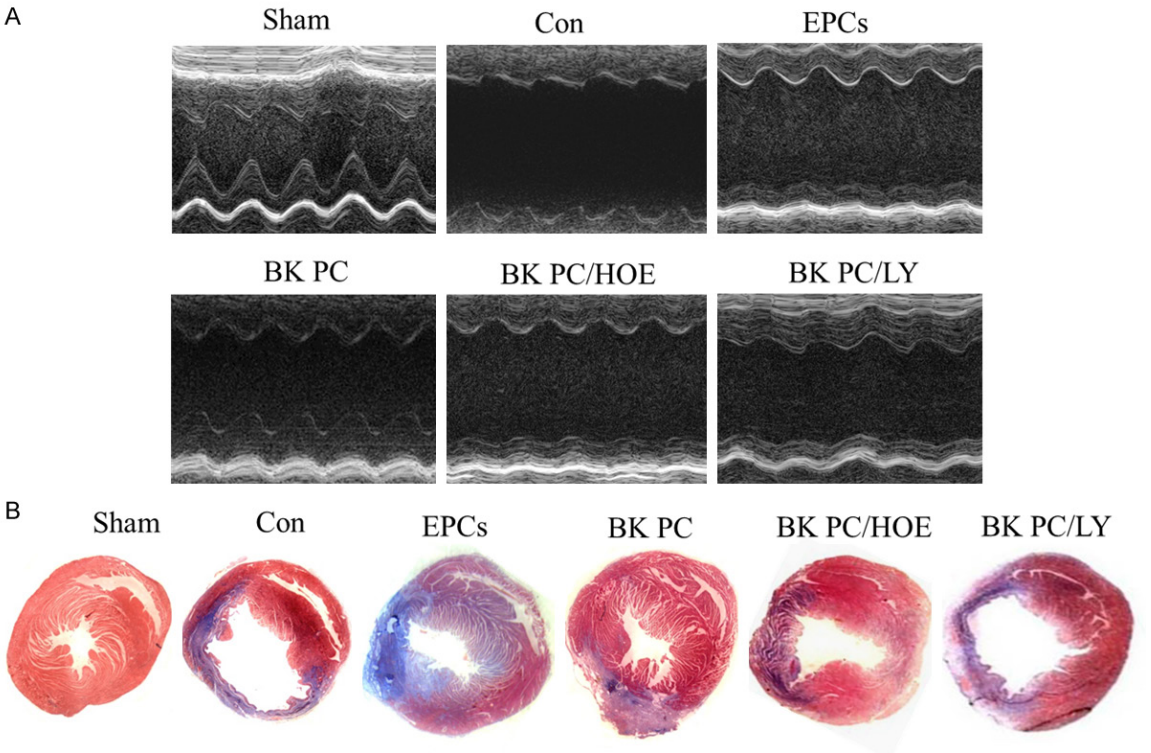

Figure 2. Measurements of cardiac function and infarct size. A. Echocardiographic measurements for determination of LV function from M-mode measurements. B. Representative Masson's trichrome-stained histological sections to measure infarct size (original magnification: 10 ×). Collagen is blue but myocardium appears red. Infarct size was quantified as the area occupied by collagen, (n = 5 for each group).

Table 1. Effects of BK preconditioning on physiological parameters, cardiac function and infarct size at 10 days following myocardial infarction

Variable	Sham	Con	EPCs	BK PC	BK PC/HOE	BK PC/LY
HW/BW (mg/g)	5.79±0.82	7.85±0.52	7.21±0.75*	6.57±0.71*,#	7.19±0.83	7.23±0.92
LVEF (%)	78.72±5.24	27.89±3.32	38.21±4.32*	48.63±4.91*,#	36.97±4.11	37.12±2.66
LVFS (%)	48.19±4.42	12.59±1.46	17.22±1.85*	27.57±2.81*,#	17.42±2.11	18.39±1.95
LVIDd (mm)	3.32±0.42	5.32±0.53	4.48±0.63*	3.48±0.35*,#	4.42±0.22	4.51±0.83
LVIDs (mm)	1.72±0.15	4.65±0.52	3.71±0.41*	2.52±0.35*,#	3.65±0.31	3.68±0.47
Infarct size (%)	0	49.21±5.12	39.05±3.74*	28.03±3.21*,#	37.64±4.43	38.78±5.18

Values are expressed as mean ± SEM. HW, heart weight; BW, body weight. LVEF, left ventricular ejection fraction; LVFS, left ventricular fractional shortening; LVIDd, left ventricular internal diameter at end-diastole; LVIDs, left ventricular internal diameter at end-systole. BK, bradykinin; PC, preconditioning; HOE, HOE140; LY, LY294002. *P < 0.01 *vs.* Con group, #P < 0.01 *vs.* EPCs group. n = 5 for each group.

tion. However, the effect of PC on cardiac function was antagonized by HOE140 and LY294002.

On the basis of Masson's trichrome staining and quantitative analysis (**Figure 2B** and **Table 1**), the infarct size in the left ventricle in the BK PC group is significantly lower than that of the Con and EPCs groups (P < 0.01) at 10 d following hEPC implantation. The effect of BK-PC on MI was abolished by HOE140 and LY294002 (P < 0.01). In addition, the heart weight/body weight ratio in the BK PC group was substantially lower than that in the other MI groups (**Table 1**).

Transplantation of BK-preconditioned hEPCs increases angiogenesis, and arteriogenesis in the peri-infarct area

Capillary density was determined by using immunohistochemical staining for CD31 in the

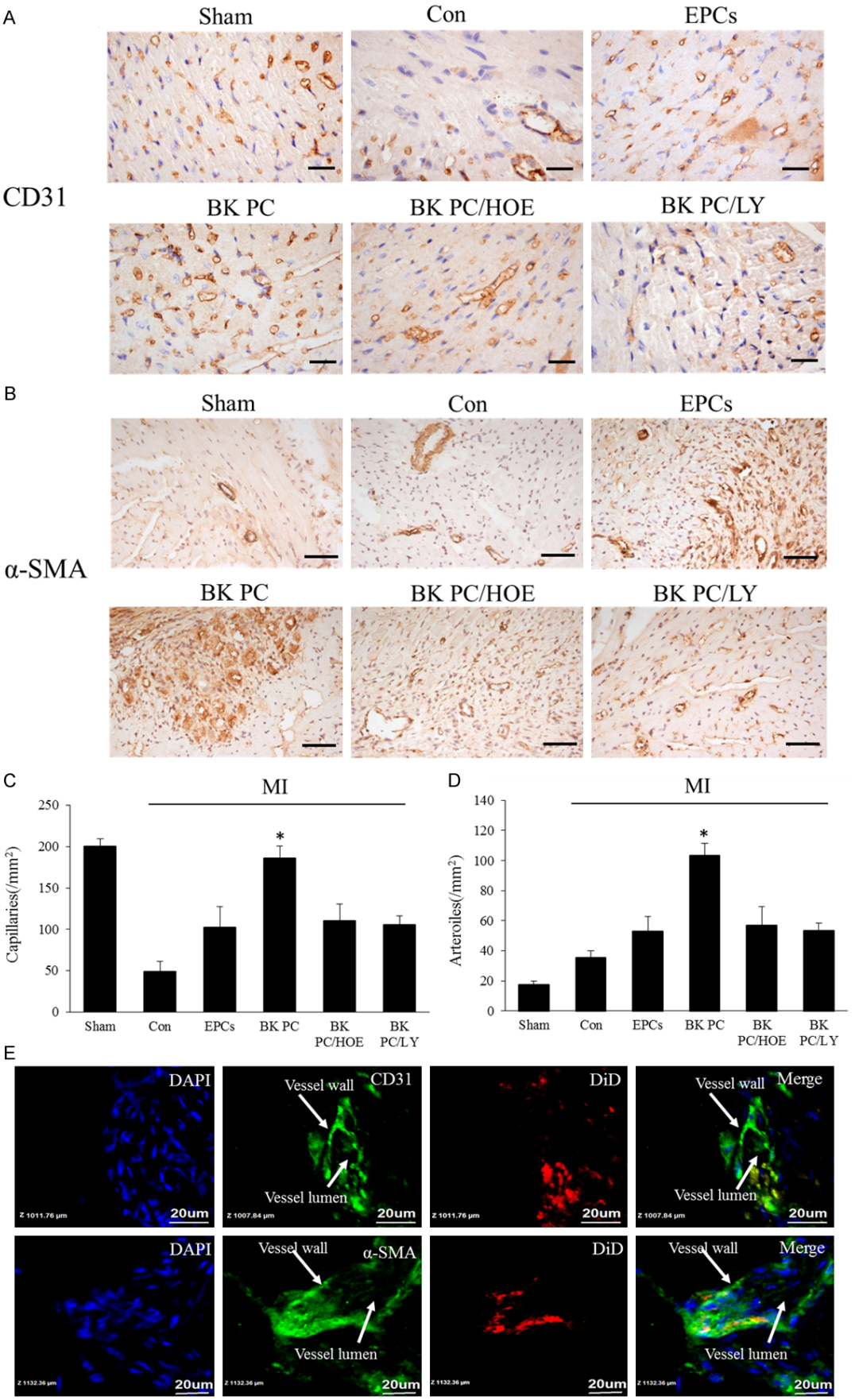
A
Sham
Con
EPCs
CD31
BK PC
BK PC/HOE
BK PC/LY
B
Sham
Con
EPCs
α-SMA
BK PC
BK PC/HOE
BK PC/LY
C
MI
Capillaries(/mm²)
250
200
150
100
50
0
Sham
Con
EPCs
BK PC
BK PC/HOE
BK PC/LY
D
MI
Arteroiles(/mm²)
140
120
100
80
60
40
20
0
Sham
Con
EPCs
BK PC
BK PC/HOE
BK PC/LY
E
DAPI
Vessel wall
CD31
Vessel lumen
DiD
Vessel wall
Merge
Vessel lumen
20um
DAPI
Vessel wall
α-SMA
Vessel lumen
DiD
Vessel wall
Merge
Vessel lumen
20um

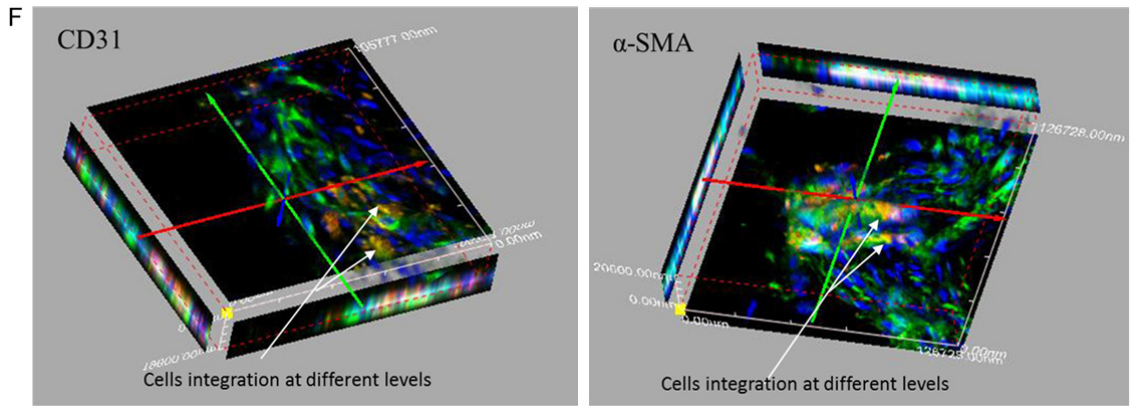

Figure 3. Effects of transplantation of BK-PC hEPCs on capillary and arteriole densities. Representative photographs of immunostaining by using CD31 (A) to identify capillaries and α-SMA (B) to identify arterioles are shown. (A: CD31, original magnification is 400 ×, bar for graph = 20 μm; B: α-SMA, original magnification is 200 ×, bar for graph = 50 μm.) Quantitative analysis of capillary density (C) and arteriole density (D) in the peri-infarct myocardium is also shown. All values are expressed as mean ± SEM (n = 5 for each group, *P < 0.01 versus other myocardial infarction groups). High-power field 2D (E) and 3D images (F) of DiD-labeled implanted hEPCs (red) and immunofluorescence staining of CD31 or α-SMA (green) at the border zone of the ischemic myocardium nuclei were counterstained with DAPI (blue). (Original magnification is 1000 ×; bar for graph = 20 μm).

peri-infarct area at 10 d following cell delivery (**Figure 3A**). BK-PC hEPC transplantation increased the capillary density in the BK PC group; this effect was completely blocked by HOE140 or LY294002. Small arterioles were clearly visible in the tissue sections stained with an antibody against α-smooth muscle actin at 10 d after cell transplantation (**Figure 3B**). Quantitative analysis shows that capillary density was significantly higher in the BK PC group than in the other groups (P < 0.01) (**Figure 3C**). while arteriolar density was significantly increased in the BK PC group compared with that in the other groups (P < 0.01) (**Figure 3D**). **Figure 3E** and **3F** show that the DiD-labeled implanted cells were incorporated into the capillaries and arterioles in the BK PC group, as assessed by a high-power confocal microscopy at the border zone of the ischemic myocardium in 2D and 3D images. These results demonstrate that transplanted cells may directly participate in angiogenesis and arteriogenesis.

PC activates the B2R-dependent Akt/eNOS phosphorylation and increases VEGF expression and NO production

To test whether BK-PC activates the B2R-dependent Akt/eNOS pathway, western blots for phosphor-Akt, total Akt, phosphor-eNOS, and total eNOS protein were performed 2 d after intramyocardial cell delivery. **Figure 4A** and **4B** show that BK-PC-hEPC transplantation on angiogenesis and arteriogenesis is associated with increased Akt and eNOS phosphorylation. HOE140 and LY294002 abolished the effects of BK-PC on both Akt and eNOS phosphorylation. Moreover, the NO levels of the BK-PC group were higher than those of the Con and EPCs groups (P < 0.05) (**Figure 4C**). However, this effect was abrogated by HOE140 and LY294002. In addition, the VEGF expression was detected following cell delivery. BK treatment significantly increased VEGF expression (**Figure 4D**). HOE140 and LY294002 abolished the effects of BK-PC on VEGF expression. These findings suggest that BK-PC-hEPC transplantation enhanced the activation of B2R-dependent Akt/eNOS and VEGF expression and subsequently increased angiogenesis and improved cardiac function in the injured myocardium.

BK-PC enhances the migration of hEPCs

Transwell assay results show that the number of migrating cells in the BK PC group significantly increased upon stimulation in the presence of 100 ng/mL SDF-1 (**Figure 5A** and **5B**). The migration activity of BK was completely blocked by HOE140 and LY294002 (P < 0.01). However, no significant differences in the number of migrating cells were noted in the Con, HOE, and LY groups.

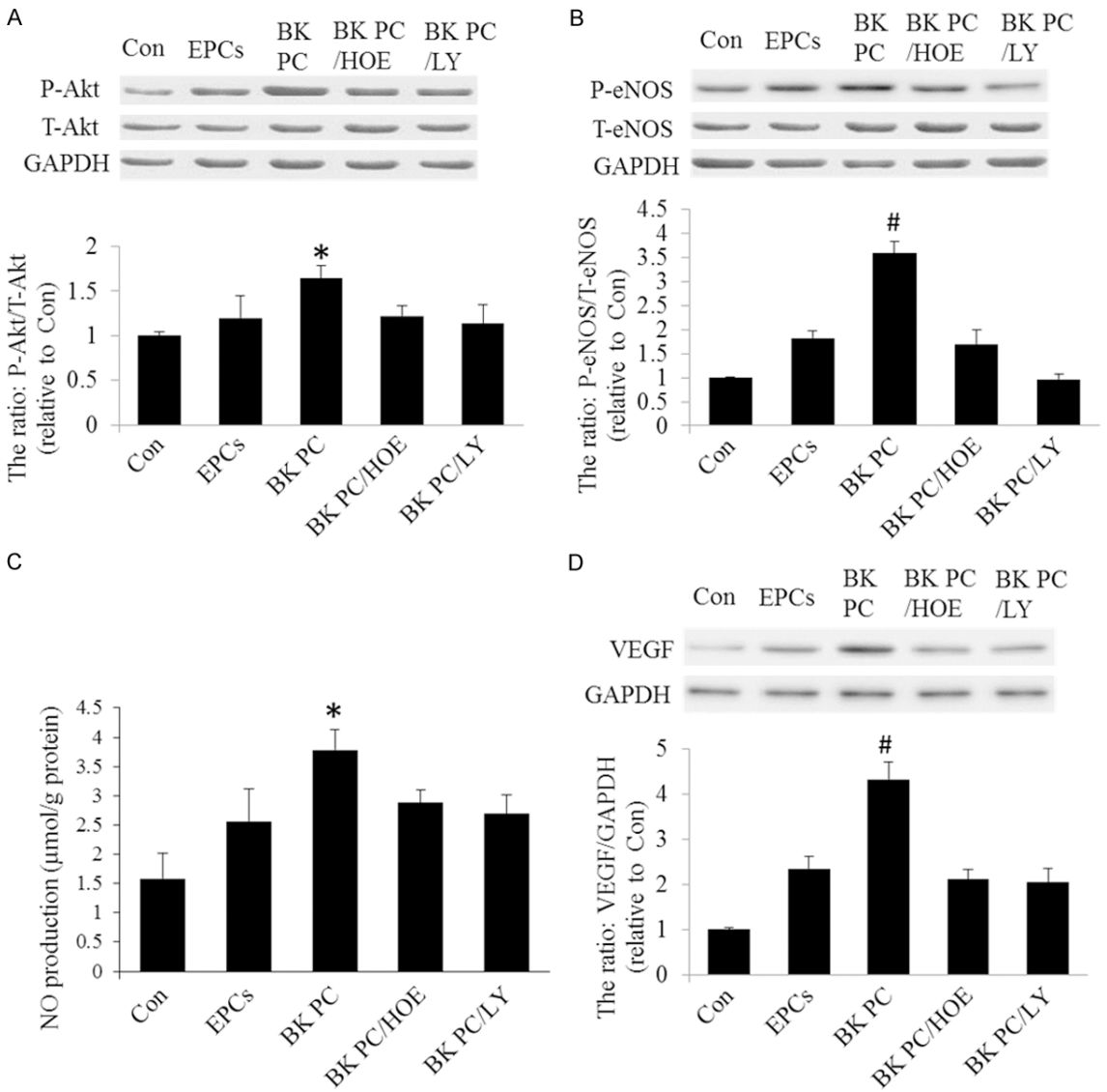

Figure 4. Effects of BK-PC-hEPC transplantation on Akt, eNOS, VEGF expression, as well as NO production. A and B. Western blots analysis to identify Akt and eNOS expressions. C. NO production in myocardial tissue. D. Western blot analysis for VEGF expression. Representative blots are shown in the upper panel, and densitometric quantitation of protein expression levels are shown as fold changes in the lower panel. All values are expressed as mean ± SEM (n = 5 for each group; $^{*}P < 0.05$ versus other myocardial infarction groups; $^{\#}P < 0.01$ versus other myocardial infarction groups).

BK-PC stimulates tube formation and enhances VEGF levels

The effect of BK-PC on the contribution of hEPCs to tube formation was studied. Quantitative analysis of the length of the tube shows that hEPCs preconditioned with BK had 2.03 times more tubes compared with that of control hEPCs ($P < 0.01$). However, this effect was abrogated by HOE140 and LY294002 ($P < 0.01$; **Figure 6A** and **6B**).

Furthermore, the VEGF levels in the supernatant in the BK PC group were higher than in the Con group ($P < 0.01$). However, the addition of HOE140 or LY294002 to the culture medium blocked these effects ($P < 0.01$; **Figure 6C**).

Discussion

BK-PC-hEPC transplantation in nude mice with MI substantially reduced infarct size and enhanced cardiac function in EF and FS. The

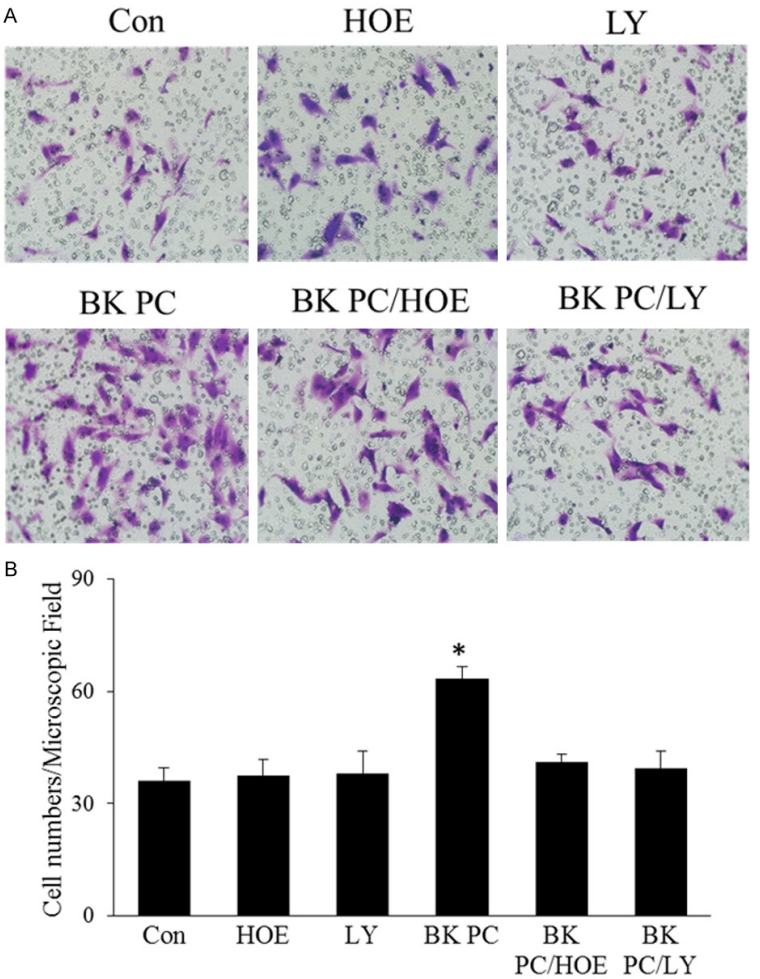

Figure 5. Effect of BK preconditioning on the migration of hEPCs. A. Representative photographs of the migrating hEPCs in the presence of 100 ng/mL SDF-1 stimulation among the six groups (original magnification: 200 ×). B. Quantitative analyses of the migrating hEPCs. All values are expressed as mean ± SEM. (n = 5 for each group; *P < 0.01 versus other groups).

diameter and volume of the left ventricle also decreased significantly. The observed angiogenesis and arteriogenesis of the transplanted cells in the infarcted tissue may also be important for the improvement of cardiac repair and function. The importance of angiogenesis and arteriogenesis in improving cardiac function has been demonstrated in previous studies [19, 20]. The present *in vitro* data show a significant increase in tube formation because of stimulation by BK-PC. Similarly, capillary density and arteriolar numbers were higher in the ischemic myocardium in the BK-PC group than in the other groups *in vivo*. These results suggest that BK-PC-hEPC transplantation improves cardiac function by increasing capillary and arteriole densities.

The significantly improved blood vessel density in the BK-PC group may be attributed to two reasons. On one hand, label-implanted cells were incorporated into capillaries and arterioles. Our result showed that BK-PC promoted hEPC migration *in vitro* and increased the integration of the transplanted cells into the vascular structures 10 d following cell delivery, based on the 2D and 3D images *in vivo*. Thus, the transplanted cells directly participated in angiogenesis and arteriogenesis, and BK-PC promoted these angiogenic effects. On the other hand, the levels of growth factors with angiogenic potential were elevated in the BK-PC group. VEGF, known as an endothelial cell-specific angiogenic factor, plays an important role in the induction and maintenance of angiogenesis [21]. The obtained data show that PC-hEPCs with BK could increase VEGF levels *in vitro*. In addition, *in vivo* data show that BK-PC-hEPC transplantation upregulated VEGF expression. This study indicates that the BK-B2R-VEGF pathway is utilized in cultured EPCs and could improve heart function through enhanced angiogenic properties. A previous study reported that B2R stimulation leads to the transactivation of KDR/Flk-1 activation, which induces tube formation [22]. Basing on these studies, we propose that PC hEPCs with BK promote neovascularization via B2R-mediated VEGF production.

Previous studies have demonstrated [23, 24] that PI3K/Akt activates downstream eNOS, induces the release of NO and eNOS phosphorylation, initiates EPC migration, and induces angiogenesis. In the present study, the PI3-kinase inhibitor LY294002 abrogated eNOS phosphorylation and reduced NO generation induced by BK-PC in the ischemic myocardium. Interestingly, PI3K/Akt activation is required for

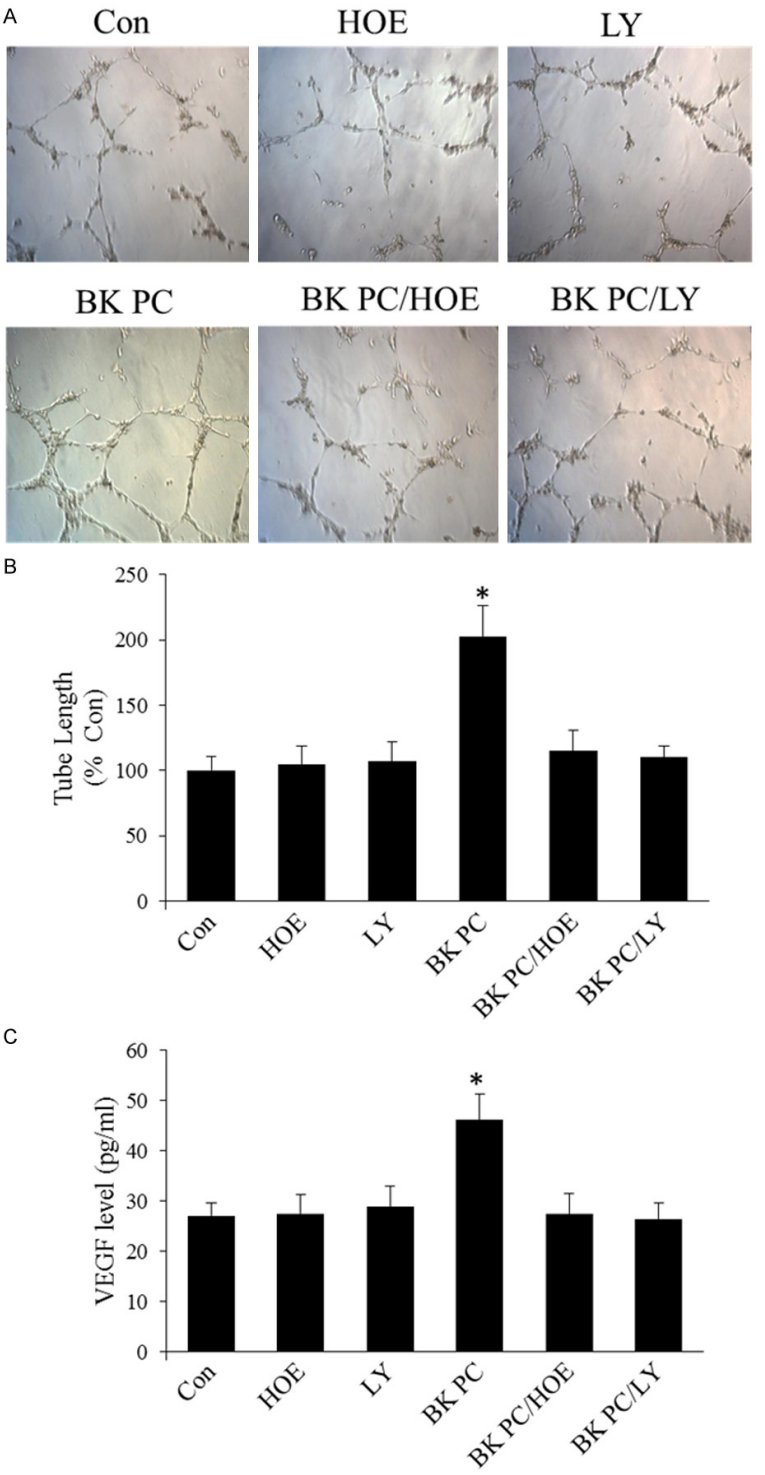

Figure 6. Effects of BK preconditioning on capillary tube formation and vascular endothelial growth factor (VEGF) levels in cultured hEPCs. A. Representative photographs of the tube formation of Matrigel-coated cultured hEPCs in various groups (original magnification: 100 ×). B. Quantitative analysis of the mean tube length, which was measured by using Image-Pro Plus and was calculated against control groups. C. Enzyme-linked immunosorbent assay of VEGF levels in culture media. All values are expressed as mean ± SEM. (n = 5 for each group; *P < 0.01 versus other groups).

angiogenesis because LY29-4002 reduces BK-PC-induced migration of hEPCs, reduces tube formation *in vitro*, and decreases capillary and arteriolar densities *in vivo*. Moreover, BK has been found to induce phosphorylation and activation of eNOS via Akt, consequently enhancing NO release [25, 26]. B2R/Akt/eNOS signaling is shown to be involved in the regulation of BK-mediated migration of human EPCs [27]. Results also show that the Akt/eNOS pathway is inhibited by HOE140, indicating that BK exerts a pro-angiogenesis effect via B2R. Collectively, the results confirm that BK-PC improves the therapeutic potential of hEPCs and subsequently increases angiogenesis following transplantation in the ischemic myocardium. This increase in angiogenesis may be associated with the increased activation of B2R-dependent Akt/eNOS.

In summary, this study demonstrates that BK-PC-hEPC transplantation reduces infarct size and improves cardiac performance by enhancing the activation of B2R-dependent Akt/eNOS and by promoting angiogenesis and arteriogenesis in the hostile environment following acute MI. Therefore, BK-PC-hEPC transplantation is a novel, cell-based therapeutic approach that can be used to improve myocardial protection in ischemic heart diseases.

Acknowledgements

This work was supported by the National Nature Science Foundation of the People's Republic of China (No. 308-

71071, No. 81070085, NO. 81470401 for Yuyu Yao; NO. 81400225 for Zulong Sheng) and the National Undergraduate Students' sInnovative Training Program (No. 1210286094).

Disclosure of conflict of interest

None.

Address correspondence to: Dr. Gen-Shan Ma or Yu-Yu Yao, Department of Cardiology, Zhongda Hospital, Medical School of Southeast University, No 87, Dingjiaqiao, Nanjing, Jiangsu, 210009, People's Republic of China. Tel: +86 25 8327 2595; Fax: +86 25 8327 2038; E-mail: magenshan@hotmail.com (GSM); yaoyuyunj@hotmail.com (YYY)

References

[1] Ferrara N, Kerbel RS. Angiogenesis as a therapeutic target. Nature 2005; 438: 967-974.

[2] Annex BH. Therapeutic angiogenesis for critical limb ischaemia. Nat Rev Cardiol 2013; 10: 387-396.

[3] Sun YY, Bai WW, Wang B, Lu XT, Xing YF, Cheng W, Liu XQ, Zhao YX. Period 2 is essential to maintain early endothelial progenitor cell function in vitro and angiogenesis after myocardial infarction in mice. J Cell Mol Med 2014; 18: 907-918.

[4] Taljaard M, Ward MR, Kutryk MJ, Courtman DW, Camack NJ, Goodman SG, Parker TG, Dick AJ, Galipeau J, Stewart DJ. Rationale and design of Enhanced Angiogenic Cell Therapy in Acute Myocardial Infarction (ENACT-AMI): the first randomized placebo-controlled trial of enhanced progenitor cell therapy for acute myocardial infarction. Am Heart J 2010; 159: 354-360.

[5] Yu P, Li Q, Liu Y, Zhang J, Seldeen K, Pang M. Pro-angiogenic efficacy of transplanting endothelial progenitor cells for treating hindlimb ischemia in hyperglycemic rabbits. J Diabetes Complications 2015; 29: 13-19.

[6] Koiwaya H, Sasaki K, Ueno T, Yokoyama S, Toyama Y, Ohtsuka M, Nakayoshi T, Mitsutake Y, Imaizumi T. Augmented neovascularization with magnetized endothelial progenitor cells in rats with hind-limb ischemia. J Mol Cell Cardiol 2011; 51: 33-40.

[7] Shen WC, Liang CJ, Wu VC, Wang SH, Young GH, Lai IR, Chien CL, Wang SM, Wu KD, Chen YL. Endothelial progenitor cells derived from Wharton's jelly of the umbilical cord reduces ischemia-induced hind limb injury in diabetic mice by inducing HIF-1α/IL-8 expression. Stem Cells Dev. 2013; 22: 1408-1418.

[8] Aicher A, Brenner W, Zuhayra M, Badorff C, Massoudi S, Assmus B, Eckey T, Henze E, Zeiher AM, Dimmeler S. Assessment of the tissue distribution of transplanted human endothelial progenitor cells by radioactive labeling. Circulation 2003; 107: 2134-2139.

[9] Kudo T, Kubo M, Katsura S, Nishimoto A, Ueno K, Samura M, Fujii Y, Hosoyama T, Hamano K. Hypoxically preconditioned human peripheral blood mononuclear cells improve blood flow in hindlimb ischemia xenograft model. Am J Transl Res 2014; 6: 570-579.

[10] Liu X, Wang JA, Ji XY, Yu SP, Wei L. Preconditioning of bone marrow mesenchymal stem cells by prolyl hydroxylase inhibition enhances cell survival and angiogenesis in vitro and after transplantation into the ischemic heart of rats. Stem Cell Res Ther 2014; 5: 111.

[11] Zemani F, Silvestre JS, Fauvel-Lafeve F, Bruel A, Vilar J, Bieche I, Laurendeau I, Galy-Fauroux I, Fischer AM, Boisson-Vidal C. Ex vivo priming of endothelial progenitor cells with SDF-1 before transplantation could increase their proangiogenic potential. Arterioscler Thromb Vasc Biol 2008; 28: 644-650.

[12] Marketou M, Kintsurashvili E, Papanicolaou KN, Lucero HA, Gavras I, Gavras H. Cardioprotective effects of a selective B(2) receptor agonist of bradykinin post-acute myocardial infarct. Am J Hypertens 2010; 23: 562-568.

[13] Li Y, Sato T. Dual signaling via protein kinase C and phosphatidylinositol 3'-kinase/Akt contributes to bradykinin B2 receptor-induced cardioprotection in guinea pig hearts. J Mol Cell Cardiol 2001; 33: 2047-2053.

[14] Baxter GF, Ebrahim Z. Role of bradykinin in preconditioning and protection of the ischaemic myocardium. Br J Pharmacol 2002; 135: 843-854.

[15] Kositprapa C, Ockaili RA, Kukreja RC. Bradykinin B2 receptor is involved in the late phase of preconditioning in rabbit heart. J Mol Cell Cardiol 2001; 33: 1355-1362.

[16] Yoshida H, Kusama Y, Kodani E, Yasutake M, Takano H, Atarashi H, Kishida H, Takano T. Pharmacological preconditioning with bradykinin affords myocardial protection through NO-dependent mechanisms. Int Heart J 2005; 46: 877-887.

[17] Sheng Z, Yao Y, Li Y, Yan F, Huang J, Ma G. Bradykinin preconditioning improves therapeutic potential of human endothelial progenitor cells in infarcted myocardium. PLoS One 2013; 8: e81505.

[18] Chen X, Gu M, Zhao X, Zheng X, Qin Y, You X. Deterioration of cardiac function after acute myocardial infarction is prevented by transplantation of modified endothelial progenitor cells overexpressing endothelial NO synthases. Cell Physiol Biochem 2013; 31: 355-365.

[19] Yuan C, Yan L, Solanki P, Vatner SF, Vatner DE, Schwarz MA. Blockade of EMAP II protects car-

diac function after chronic myocardial infarction by inducing angiogenesis. J Mol Cell Cardiol 2015; 79: 224-231.

[20] Besnier M, Galaup A, Nicol L, Henry JP, Coquerel D, Gueret A, Mulder P, Brakenhielm E, Thuillez C, Germain S, Richard V, Ouvrard-Pascaud A. Enhanced angiogenesis and increased cardiac perfusion after myocardial infarction in protein tyrosine phosphatase 1B-deficient mice. FASEB J 2014; 28: 3351-3361.

[21] Baggott RR, Alfranca A, López-Maderuelo D, Mohamed TM, Escolano A, Oller J, Ornes BC, Kurusamy S, Rowther FB, Brown JE, Oceandy D, Cartwright EJ, Wang W, Gómez-del Arco P, Martínez-Martínez S, Neyses L, Redondo JM, Armesilla AL. Plasma membrane calcium ATPase isoform 4 inhibits vascular endothelial growth factor-mediated angiogenesis through interaction with calcineurin. Arterioscler Thromb Vasc Biol 2014; 34: 2310-2320.

[22] Miura S, Matsuo Y, Saku K. Transactivation of KDR/Flk-1 by the B2 receptor induces tube formation in human coronary endothelial cells. Hypertension 2003; 41: 1118-1123.

[23] Madeddu P, Kraenkel N, Barcelos LS, Siragusa M, Campagnolo P, Oikawa A, Caporali A, Herman A, Azzolino O, Barberis L, Perino A, Damilano F, Emanueli C, Hirsch E. Phosphoinositide 3-kinase gamma gene knockout impairs postischemic neovascularization and endothelial progenitor cell functions. Arterioscler Thromb Vasc Biol 2008; 28: 68-76.

[24] Aicher A, Heeschen C, Mildner-Rihm C, Urbich C, Ihling C, Technau-Ihling K, Zeiher AM, Dimmeler S. Essential role of endothelial nitric oxide synthase for mobilization of stem and progenitor cells. Nat Med 2003; 9: 1370-1376.

[25] Bell RM, Yellon DM. Bradykinin limits infarction when administered as an adjunct to reperfusion in mouse heart: the role of PI3K, Akt and eNOS. J Mol Cell Cardiol 2003; 35: 185-193.

[26] Feng J, Li H, Rosenkranz ER. Bradykinin protects the rabbit heart after cardioplegic ischemia via NO-dependent pathways. Ann Thorac Surg 2000; 70: 2119-2124.

[27] Kränkel N, Katare RG, Siragusa M, Barcelos LS, Campagnolo P, Mangialardi G, Fortunato O, Spinetti G, Tran N, Zacharowski K, Wojakowski W, Mroz I, Herman A, Manning Fox JE, MacDonald PE, Schanstra JP, Bascands JL, Ascione R, Angelini G, Emanueli C, Madeddu P. Role of kinin B2 receptor signaling in the recruitment of circulating progenitor cells with neovascularization potential. Circ Res 2008; 103: 1335-1343.